CrossMark

ORIGINAL RESEARCH PAPER

Cost assessment of isolation technique applied to a benchmark bridge with soil structure interaction

Davide Forcellini[1]

Abstract Bridges are lifeline structures acting as an important link in surface transportation network and their collapse under seismic excitations affects social and civil functionality. Historical bridge seismic collapses under earthquake actions have proved the significant role of soil structure interaction. The paper aims at evaluating bridge protection and seismic strengthening applying isolation technique. It is based on the application of a Performance-Based Earthquake Engineering methodology, introduced by the Pacific Earthquake Engineering Research Center. The study presents a representative two—span bridge with several isolated configurations as affected by soil deformability. Isolation technique contribution is assessed in terms of costs quantities with peak ground acceleration levels. The study can be considered a first attempt to evaluate seismic effects of SSI by taking into account economic performance.

Keywords Earthquake · Bridge · Isolation · PBEE · SSI · Non-linearity

1 Introduction

Seismic assessment is fundamentally important for both pre-earthquake and post-earthquake decision-making analysis (Forcellini 2016). On the one hand, it aims to make better-informed decisions on allocation of resources for retrofit, design and assessing redundancy of a network. On the other hand, seismic evaluation is fundamental for post-earthquake repair and network capacity management. Particularly, since the Northridge Earthquake, research studies, such as Caltrans (1994), have proved the significant role of soil structure interaction (SSI) on the seismic response of bridges. In this regard, several studies focusing on SSI for seismically isolated bridge structures have been available in literature, such as

✉ Davide Forcellini
davide.forcellini@unirsm.sm

[1] University of San Marino, 47890 San Marino, Republic of San Marino

Thakkar and Maheshwari (1995), Chaudhary et al. (2001), Liao et al. (2000), Kunde and Jangid (2003), Vlassis and Spyrakos (2001), Tongaonkar and Jangid (2003), Lee et al. (2003) and the most recent Ucak and Tsopelas (2008).

Past earthquakes all over the world have proved that bridge damage occurs primarily to the piers, which may in turn result in the collapse of the bridge spans. Therefore, pier protection should be considered one of the most important goals for bridge protection or strengthening against earthquakes. In this regard, seismic isolation is conceivably one of the most promising alternatives especially in post-earthquake rehabilitation as shown in Makris and Zhang (2004) and Morgan and Mahin (2011). This technique is based on uncoupling structures from the damaging components thanks to a mechanism that provides flexibility and energy absorption capacity at the same time. In particular, isolating the deck from the bridge substructure, significantly reduces the deck accelerations and consequently the forces transmitted to the piers. This behavior can be modified by soil deformability and energy dissipation in the ground. In particular, Vlassis and Spyrakos (2001) and Tongaonkar and Jangid (2003) reached the conclusion that considering SSI generally improves safety and design costs. In these studies, isolation systems were modelled with linear elastic behaviour. Ucak and Tsopelas (2008) contrasted these results considering two seismically isolated bridges founded on soft soil through pile group foundations and adopting a non-linear hysteretic behaviour as isolation system. The above paper assesses the importance of damping and foundation impedances on SSI, when a linear-elastic foundation system is modelled with springs, dashpots and artificial masses. The present study aims at overcoming the previous contributions by considering a 3D soil-structure system of a benchmark bridge configuration. The adopted approach allows modelling soil hysteretic elasto-plastic shear response (including permanent deformations) and thus damping foundation impedances by considering a Von Mises multi-surface kinematic plasticity model.

Moreover, in the past 20 years, isolation applications in bridge engineering have been developed thanks to new code approaches built on performance-based design (PBD). The principle consists in evaluating various design alternatives and their ability to reliably achieve targeted performance goals. The paper aims at evaluating the relationships among various characteristics of a benchmark bridge, including ground motion, superstructure, foundation and isolation devices. The target is to assess the performance of various isolated configurations adopting a Performance-Based Earthquake Engineering (PBEE) methodology developed by the Pacific Earthquake Engineering Research (PEER) Center (http://peer.berkeley.edu). In particular, PBEE methodology (Mackie et al. 2008, 2010a) aims at assessing structural performances in terms of the probability of exceeding threshold values of socio-economic decision variables (DVs) in the seismic hazard environment. The PEER PBEE framework is fundamentally based on the definition of several performance groups (PGs) and built on the association of various structural and non-structural components for related repair work. They contain a collection of components that reflect global-level indicators of structural performance and repair-level decisions. For more details on the definition variables, see Mackie et al. (2010a); for numerical implementations, see Mackie et al. (2010b) and Lu et al. (2011).

This study can be considered one of the relatively few attempts that applies PBEE methodology in bridge and infrastructure engineering taking into consideration both SSI and isolation technique. In particular, the aim is to provide a contribution for seismic assessment by comparing two different types of isolation devices (elastomeric and sliding bearings) in the longitudinal direction. In particular, several configurations have been studied depending on where the devices have been placed. The study aims at evaluate

structural response taking into account economic performance based on assessment of repair costs.

2 Case study

The case study consists of an original benchmark bridge studied at University of California (Mackie et al. 2012) and intended to be representative of the prevalent ordinary construction types for California highways designed according to the Caltrans Seismic Design Criteria and classified as Ordinary Standard Bridge (OSBs). The properties were derived from the Type 1 class of bridge design (Ketchum et al. 2004). The bridge is a 90 m long, 2-span structure, supported by one circular column (1.22 m diameter), 6.70 m above grade. The deck is 11.90 m wide and 1.80 m deep and the weight is 130.30 kN/m. Each abutment is 25 m long with 30,000 kN as total weight (see Fig. 1).

The original configuration has been equipped with isolation devices, as shown in Table 1. First of all, the study considers the original model (I-01) with isolated abutments, roughly representative of a rubber bearing isolator, currently used in design. In order to increase bridge flexibility, the original connection between the top of the column and the deck has been removed and performed with two different types of isolators. In I-02 model, isolation is reproduced with a linear elastic behaviour representative of several bearing isolators. In I-03 model, isolators on the top of the column and on each abutment have been performed with a two-spring model (Kelly 1997, 2003; Forcellini and Kelly 2014) as to perform a sliding isolation system with a non-linear behaviour.

In order to reproduce typical California seismicity, the study employs 100 input motions, selected from the PEER NGA database (http://peer.berkeley.edu/nga/) and consisting of 3D input ground motions triplets. Each motion is composed of 3 perpendicular acceleration time history components (2 lateral and 1 vertical). Motions are divided into 5 bins of 20 motions each with characteristics: moment magnitude (Mw) 6.5–7.2 and closest distance (R) 15-30 km, Mw 6.5–7.2 and R 30–60 km, Mw 5.8–6.5 and R 15–30 km, Mw 5.8–6.5 and R 30–60 km, and Mw 5.8–7.2 and R 0–15 km. The NGA database has been chosen because the frequencies of the input motions are close to the fundamental
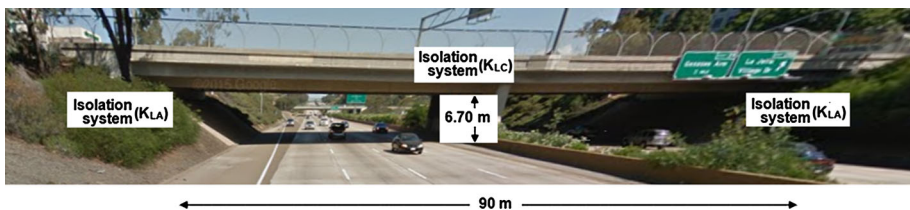

Fig. 1 Benchmark bridge

Table 1 Data models

	KL_A (kN/m)	KL_C (kN/m)	Isolation	Analytical model
I-01	1460	Fixed	Abutment isolation	Linear
I-02	1460	2920	Full isolation	Linear
I-03	NL	NL	Full isolation	Two-spring model
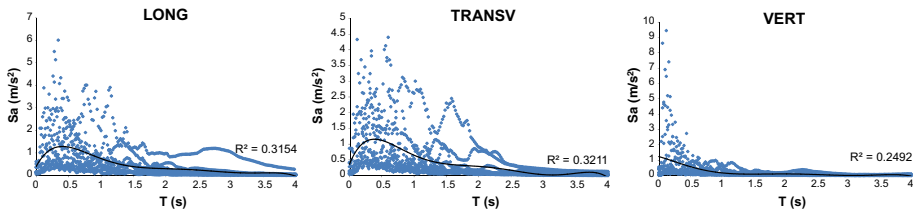
Fig. 2 NGA-input motions (spectra)
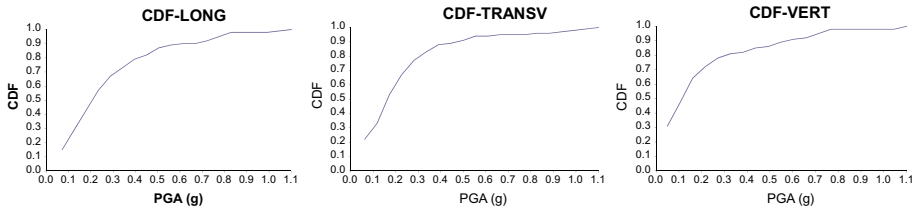
Fig. 3 NGA-input motions (CDFs)

Table 2 Soil models

	Hard	Stiff clay	Medium clay	Soft clay
Mass density (t/m^3)	2.1	2.0	1.5	1.3
Reference shear modul (kPa)	2.10×10^6	3.70×10^5	6.00×10^4	1.30×10^4
Reference bulk modul (kPa)	1.05×10^7	1.85×10^6	3.00×10^5	6.80×10^4
Cohesion (kPa)	180	75	37	18
Shear wave velocity (m/s)	1000	430	200	100
Characteristic site period (s)	0.08	0.186	0.40	0.80

frequencies of the system, in order to affect significantly its seismic performance. In particular, Figs. 2 and 3 show the trend lines (polynomial approximation) and the cumulative density functions (CDFs) for the 100 motions (longitudinal, transversal and vertical directions).

Finally, SSI effects have been assessed by increasing soil deformability from a hard soil (simulating fixed conditions and consequently neglecting SSI effects) to three cohesive soils representative of stiff, medium and soft clays, as presented in Table 2.

2.1 PBEE methodology

PBEE framework is fundamentally based on the application of the total probability theorem to disaggregate the problem into several intermediate probabilistic models that involve intermediate variables, such as the definition of several PGs. They are based on the association of the various structural and non-structural components for related repair work and they contain a collection of components that reflect global-level indicators of structural performance and repair-level decisions. Therefore, PGs are not necessarily the same as the individual load-resisting structural components. In particular, the original platform is built with 11 PGs, based on commonly used repair methods and the aggregation of decision data,

mainly taken from typical pre-stressed, single-column bent, multi-span, box girder bridges in California. This study assesses the coupled soil-structure system focusing on the longitudinal drift ratio (PG1) and the relative longitudinal displacement between the deck end and the abutment (PG3), representing the column and the abutments damage, respectively. These quantities have been calculated by a probabilistic procedure called the local linearization repair cost and time methodology (LLRCAT) and developed by Mackie et al. (2008). In particular, this methodology involves local linearization of the Q-DM model, extension from Q to repair cost and repair time, and a structural data. LLRRCAT methodology is based on the closed-form "Fourway method" (Mackie and Stojadinovic 2006), piecewise power-law approach, and Monte Carlo simulations. Results are expressed in the form of repair cost ratio (RCR) defined as the percentage ratio of the repair cost over the replacement cost. The latter does not include demolition cost. Costs have been calculated from the repair quantities taken from Caltrans bridge database used for planning purposes. They are based on the deck and type of construction and parameterized in terms of basic bridge geometry and properties so that they can be used to extrapolate loss modelling. Monetary costs have been adjusted to 2007 values, based on Caltrans cost index data.

2.2 Finite element model

The finite element model (Fig. 4) has been built with OpenSees (Open System for Earthquake Engineering Simulation) that allows high level of advanced capabilities for modelling and analysing non-linear responses of systems using a wide range of material models, elements and solution algorithms.

2.3 Soil model

The 3D mesh (Fig. 4) aims at performing tridimensional SSI analyses, by applying OpenSees potentialities. Soil is modelled with a 200 × 200 m, 20 m mesh built up with 6360 modes and 5330 non-linear solid brick elements called "Bbar brick" (Mazzoni et al. 2009). Mesh dimensions have been determined following the suggestions indicated in
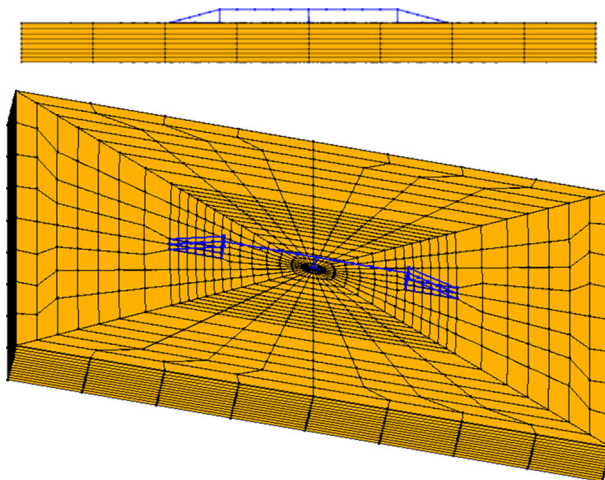

Fig. 4 Soil-structure finite element model: 3D and vertical view

Attewell and Farmer ([1973](#)) and Jesmani et al. ([2012](#)). Discretization is built up with relatively small elements around the bridge and gradually larger toward the outer mesh boundaries (as shown in Fig. [4](#)). OpenSees is able to simulate real wave propagation by adopting realistic boundaries that have been located as far as possible from the structure as to decrease any effect on the response. In particular, at any special location, symmetry conditions can be adopted and periodic boundaries (Law and Lam [2001](#)) have been considered. Displacement degrees of freedom of the left and right boundary nodes have been tied together both longitudinally and vertically using the penalty method. In this regard, base and lateral boundaries have been modelled to be impervious, as to represent a small section of a presumably infinite (or at least very large) soil domain and allowing the seismic energy to be removed from the site itself, as shown in Forcellini and Gobbi ([2015](#)).

Soil damping has been modelled by considering a nonlinear material (Parra [1996](#); Yang et al. [2003](#); Elgamal et al. [2003](#)), allowing to take into account the dynamic nature of the phenomena (such as hysteretic response and radiation damping). In particular, a Von Mises multi-surface (Iwan [1967](#); Mroz [1967](#)) kinematic plasticity model has been applied in order to reproduce the soil hysteretic elasto-plastic shear response (including permanent deformations). The model is developed within the framework of multi-yield-surface plasticity (Prevost [1985](#)) and focusing on controlling the magnitude of cycle-by-cycle permanent shear strain accumulation (see Parra [1996](#); Yang et al. [2003](#)). In particular, plasticity is exhibited only in the deviatoric stress–strain response. The volumetric stress–strain response is linear-elastic and is independent of the deviatoric response. This constitutive model is able to simulate monotonic or cyclic response of materials whose shear behavior is insensitive to the confinement change. Plasticity is formulated based on the multi-surface (nested surfaces) concept, with an appropriate non-associative flow rule (Prevost [1985](#); Dafalias [1986](#); Boussshine et al. [2001](#); Nemat-Nasser and Zhang [2002](#); Radi et al. [2002](#)). In detail, flow rule deviatoric component is associative, while non-associativity is restricted to the volumetric component. The nonlinear shear stress strain back-bone curve is represented by the hyperbolic relation (Kondner [1963](#)), defined by the two material constants, low-strain shear modulus and ultimate shear strength. Soil has been modelled with three clay materials called Pressure Independent Multiyield (Mazzoni et al. [2009](#)) built up with representative parameters shown in Table [2](#). In order to introduce these parameters inside the code, shear strain Vs shear stress relationships (backbone curves) have been implemented. Figure [5](#) shows the applied backbone curves for the considered soils (named HARD, STIFF, MEDIUM and SOFT in the figure).

Characteristic site periods have been calculated by assuming a uniform and damped soil (Kramer [1996](#)). The selected materials have been calibrated in order to assess different soil behaviour, such as amplitude-dependent amplification (or deamplification) because of soil nonlinearity and hysteretic damping and the gradual accumulation of ground deformation (laterally and vertically) that can influence residual response on the column and the abutments damage.

In detail, a hard soil (shear velocity equal to 1000 m/s) is applied in order to reproduce rigid base conditions (SSI neglected). Table [2](#) shows that the hard soil has been calibrated in order to be much stiffer than the structure and thus to be able to neglect SSI effects. In order to verify this assumption, the acceleration input at the base of the mesh was compared to the accelerations at the top of the layers (that propagates at the base of the columns and o the abutments) and they were found identical. On the other hand, Table [2](#) verifies that soft soil characteristic period is close to the structural fundamental period, indicating that SSI effects should not be neglected. In this regard, Table [3](#) shows how the first two natural periods of the 3 considered configurations vary with soil conditions. In order to
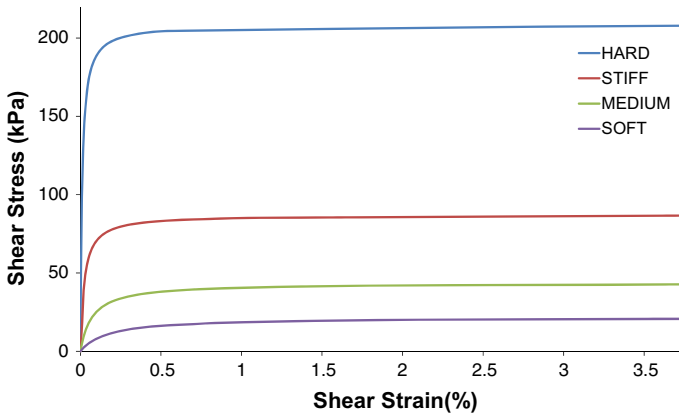
Fig. 5 Backbone curves (HARD, STIFF, MEDIUM, SOFT)

Table 3 Natural Periods (first and second) of the considered configurations (I-01, I-02, I-03) in correspondence with different soil conditions (HARD, STIFF, MEDIUM, SOFT)

Model	Hard		Stiff		Medium		Soft	
	T1 (s)	T2 (s)	T1 (s)	T2 (s)	T1 (s)	T2 (s)	T1 (s)	T2 (s)
I-01	0.811	0.506	0.809	0.505	0.893	0.510	1.020	0.800
I-02	0.843	0.690	0.855	0.694	0.880	0.719	1.000	0.800
I-03	0.813	0.527	0.866	0.527	0.926	0.529	1.130	0.805

assess local soil effects, input motions have been applied to the 3D soil mesh with different deformability conditions.

Figure 6 shows transfer functions for a selected input motion for all the considered soils. In particular, the longitudinal (Fig. 6a) and transversal components (Fig. 6b) verify the reproduction of the vibrational characteristics of the soil layer for each homogeneous soil medium examined in the paper. The peak values are shown to be close to the characteristic site periods named with "linear" in the figures and calculated by the linear formulation $T = 4 H/Vs$ (Kramer 1996). H is the height of the soil layer and Vs the shear wave velocity of each layer (Table 2).

2.4 Bridge model

Figure 7 shows the structural model of the benchmark bridge. The reinforced concrete column is modelled with non-linear forced-based beam-column elements and fiber cross section, with 0.2 rad/m as the maximum curvature (Fig. 8). The column has been settled on a single Type I Caltrans pile shaft (20 m length) assumed to have cross section and reinforcement continuous with the column above and below grade.

The deck is assumed to be capacity designed so that it is able to respond in the elastic range. This assumption is reasonable since the isolation systems have been designed in order to perform their function. It was modelled using two-noded beam-column elements (with cross Area of 5.72 m^2, transversal inertia 2.81 m^4 and vertical inertia 53.9 m^4)
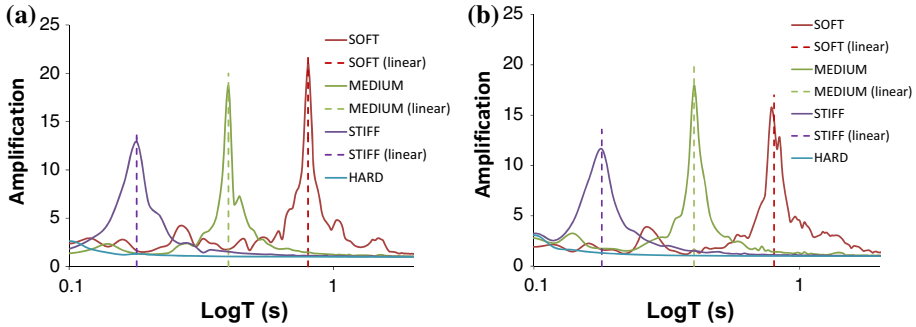
(a)

(b)

Fig. 6 Local effects assessment—transfer functions (free field conditions): comparison between the performed soils with the characteristic site periods (linear, Kramer 1996)
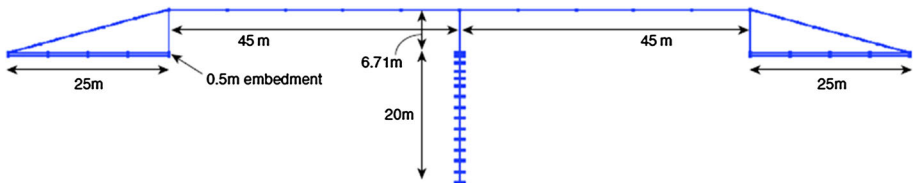

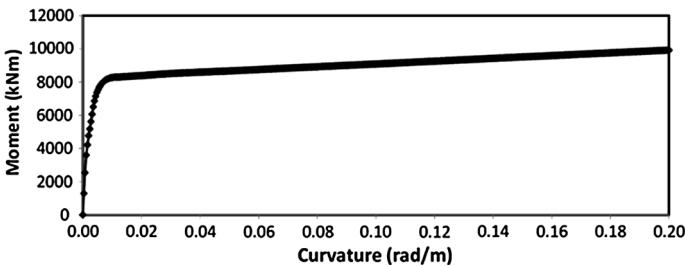Fig. 7 Bridge mesh details: vertical view

Fig. 8 Moment—curvature diagram

discretized into separate elastic beam-column elements. Longitudinal behaviour is described by the first two natural periods (0.811 and 0.506 s respectively), shown in Fig. 9. In order to prove the validity of the previous hard soil conditions ($V_s = 1000$ m/s), eigenvalues have been calculated and compared with those obtained by a software (SAP2000) able to simulate fixed base conditions and generally adopted in professional designs. The first two natural periods were found to be 0.791 and 0.523 s respectively.

The approach ramp model connects the bridge longitudinal boundaries to the ground using a trapezoidal arrangement of rigid link elements that extends 0.5 m into the soil domain below the abutments (Figs. 4, 7). The rigid link assembly captures the embankment and approach geometry and permits interaction with the bridge at its ends, including the potential embankment settlement into the surrounding soil. The abutment model provides the interface between the approach ramps and the bridge ends in order to simulate the concrete type abutment configuration, studied in this paper. System behaviour is based on
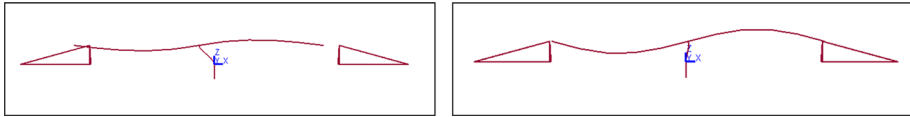
Fig. 9 1st ($T_1 = 0.811$ s) and 2nd ($T_2 = 0.506$ s) shape mode, benchmark bridge modelled with OpenSees

the response of the elastomeric bearing pads, gap, abutment back wall, abutment piles, and soil backfill material. Prior to gap closure, the superstructure forces are transmitted through the elastomeric bearing pads to the stem wall, and subsequently to the piles and backfill, in a series system. After gap closure, the superstructure bears directly on the abutment back wall and begins to mobilize the passive backfill pressure. The abutment is assumed to have a nominal mass proportional to the superstructure dead load, including a contribution from structural concrete.

Connections between the abutments and the deck are performed with a model developed by Mackie and Stojadinovic (2006) which includes sophisticated longitudinal, transverse, and vertical pads able to simulate nonlinear abutment response. The participating mass has been assigned in order to represent typical concrete abutments and mobilized embankment soil. A system of rigid elements was oriented in the transverse bridge direction. Their stiffness was set big enough in order to be considered infinite. These elements are connected with discrete zero-length elements representing bearing pads able to reproduce the response as the superstructure rotates about the vertical bridge axis. Longitudinal elastomeric bearing pad response and gap closure behavior were modelled in order to represent the isolation devices. Vertical stiffness was considered sufficiently big in order to be considered fixed. Two bearing pads in symmetrical positions were implemented, according to plan locations. The properties of bearing pads are detailed in the following paragraph. The interface between the column and the soil has been modelled following the previous research studies (Elgamal et al. 2009; Mackie et al. 2012). In particular, rigid beam-column links, normal to the pile longitudinal axis, were used to represent the geometric space occupied by the pile. The soil domain 3D brick elements are connected to the column at the outer nodes of these rigid links using the equalDOF constraint in OpenSees for translations only that connects two separate points (one belonging to the structure and the second to the soil) and imposes equality of displacements. The system is able to capture the interaction between the column and the ground, including the potential settlement into the surrounding soil.

2.5 Isolated configurations

The study performs the isolator in the longitudinal direction only. The bearings have been modelled very stiff in the other directions (vertical and transversal). The two types of isolation devices (elastomeric bearings and frictional/sliding bearings) performed here, are applied in many countries all over the world, as shown in Kunde and Jangid (2003). In particular, Table 1 shows the studied several configurations, depending on where the devices have been placed (over the column as well as at the abutments).

First of all, the study considers I-01 model where abutments have been isolated with two Soft Damping Rubber Bearings (HDS 650 × 337) with modulus of elasticity G = 0.4 Mpa and equivalent viscous damping $\xi = 10$ % from ALGA S.p.A. (http://www.alga.it). They have been modelled with 2 simple elastic springs (730 kN/m each). A second
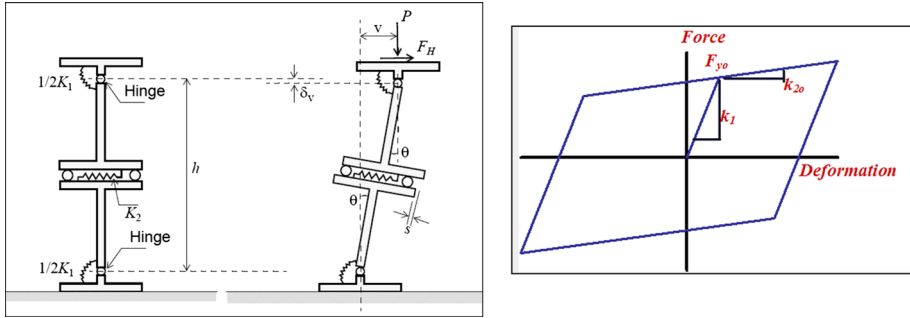
Fig. 10 Simplified two-spring model (I-NL) element and model (Mazzoni et al. 2009)

model (I-02 model) adopts the same rubber bearing devices (HDS 650 × 337) at the top of the column (2920 kN/m totally) and at the abutments (730 kN/m each), in order to simulate a fully isolated configuration. Finally, a third model (I-03 model) applies APS 3000/800 sliding isolators at the top of the column and at the abutments. They are modelled with a simplified two-spring model (Fig. 10) built with two rigid elements connected by moment springs across hinges at the top and bottom and by shear springs and frictionless rollers at mid-height. The kinematics of the model is described by shear displacements and relative rotations. The tested non-linear behaviour has been implemented with a bilinear spring controlled by several parameters such as the initial bending stiffness $k_1/2$, yield strength F_{yo} and post-yield stiffness k_{2o} (Fig. 10, details in Ryan et al. 2005; Mazzoni et al. 2009). In the model these parameters have been set 28,500 kN/m, 287 kN and 166.67 kN/m, respectively.

3 PBEE results

Result from previous studies (Elgamal et al. 2009, 2012; Forcellini et al. 2012; Forcellini and Banfi 2013; Forcellini 2014) show that the main contributions can be described by two PGs, identified with longitudinal drift ratio (PG1) and relative longitudinal displacements between deck end and abutments (PG3), representing column and abutment damage, respectively. In this paragraph, the response of hard soil (Figs. 11, 12, 13) and deformable soils (Figs. 14, 15, 16) have been shown. The figures consider PGA as the intensity measure in order to reproduce the system performance.

3.1 Hard soil results

Figure 11 shows costs connected to column damage (PG1). Models are affected by horizontal and vertical displacements that affect column damage and thus total RCRs. In detail, full isolated configuration (I-02 and I-03 models) responses show lower costs if compared with the original I-01 model. This is due to the decoupled behaviour between bridge and soil, operated by isolation devices. In particular, column isolation effectiveness increases with high values of PGA. For example, in correspondence with PGA equal to 0.70 g, I-02 and I-03 results are around 31.6 and 43.5 % respectively, less than the values obtained for the I-01 configuration. Finally, the I-02 model seems to work better than the I-03 model.
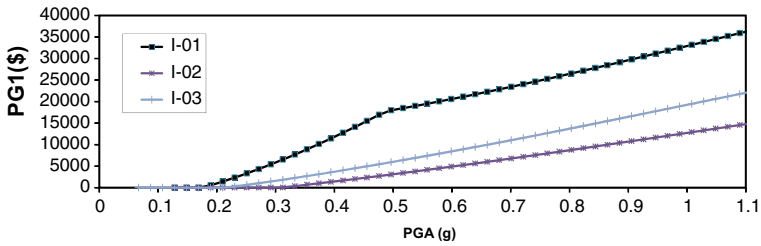
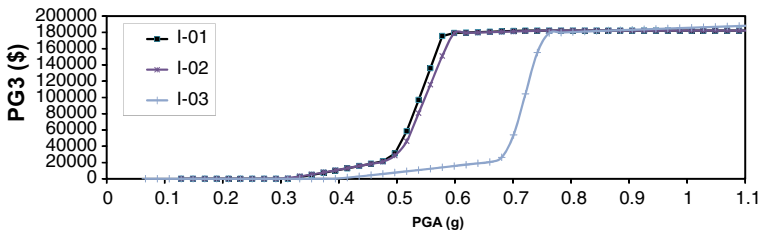**Fig. 11** Maximum longitudinal drift ratio (Column)—PG1 (hard soil)

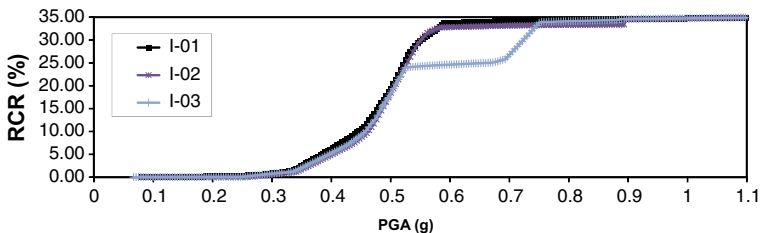**Fig. 12** Maximum longitudinal relative deck end–abutment displacement—PG3 (hard soil)

Fig. 13 Total repair cost ratio (%) results (hard soil)

The same considerations can be taken from Table 4, showing maximum displacements in correspondence with the column (three directions).

Figure 12 shows the effects of isolation on the abutment damage (PG3). I-01 and I-02 responses are close to each other demonstrating that column isolation has negligible effects on energy dissipation and thus on reducing abutment damage, when linear assumptions are considered. On the contrary, the I-03 model is shown to have a significant reduction in the range of PGA between 0.40 and 0.70 g. In particular, in correspondence with PGA equal to 0.70 g, I-03 model costs are around 14.3 % lower than those performed for I-01 and I-02 configurations. This reduction shows non-linear effectiveness in reducing the damage transferred to abutments between 0.40 and 0.70 g. The same considerations are shown in Table 5 that shows maximum displacements in correspondence with the abutments (three directions). Therefore, it can be deduced that linear assumptions do not properly reproduce the behaviour of a sliding system.

Figure 13 shows seismic performances in terms of total RCR. Comparing Figs. 11 and 12, it is shown that the response is due mainly to PG3 contribution. Therefore, column
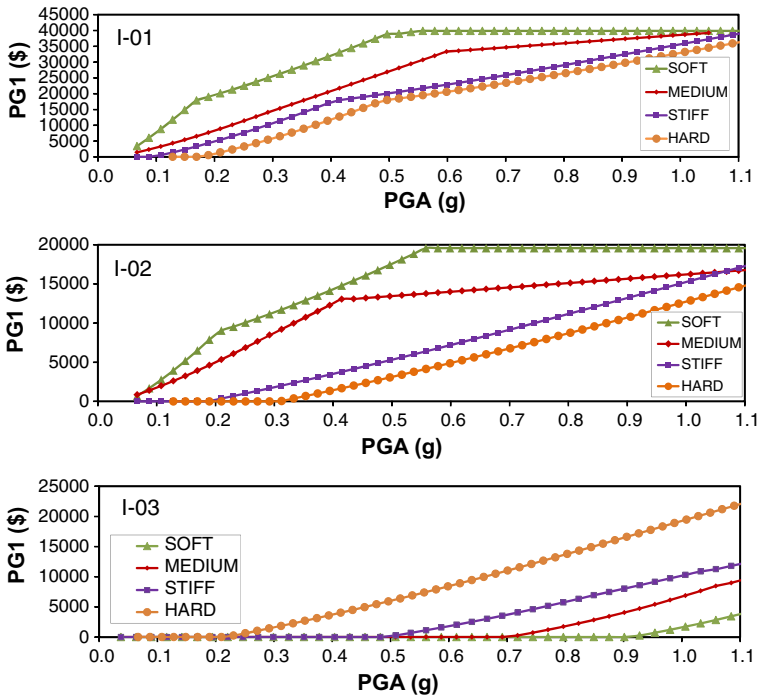
Fig. 14 Maximum longitudinal drift ratio (column)—PG1 results

isolation does not significantly affect total costs. This means that saving the column does not mean reducing the costs of the structure and thus improving system performance. Nonlinear contribution is represented by a significant reduction of total repair costs between 0.50 g and 0.80 g PGA values.

3.2 SSI results

Figures 14, 15, 16 show the influence of soil deformability considering column damage (PG1), on the abutment costs (PG3) and on the RCR for the three isolated configurations.

Figure 14 shows different behaviours of column damage (PG1) for the configurations. For I-01 and I-02 models, soil deformability is detrimental because soft soil needs lower values of PGA to register damage to the column. In particular, isolation on the top of the column is able to protect the column for about 50 % of the original damage (I-02 values are around 50 % less than those of I-01). On the contrary, I-03 response shows that column damage is reduced when soil deformability increases. This is due to the non-linear devices that are able to absorb the strain transmitted to the column and thus to the soil. In particular, when the shear strain induced to the earthquake becomes significantly high, it starts to affect the soil-structure system, in particular the column. Thanks to the mutual effects of non-linear devices and high deformability of the soil, soft soil needs higher value of PGA to register damage in the column. Therefore, when the bridge is equipped with non-linear isolators, soft soil seems to absorb the effects of seismic waves in correspondence with the base of the column.
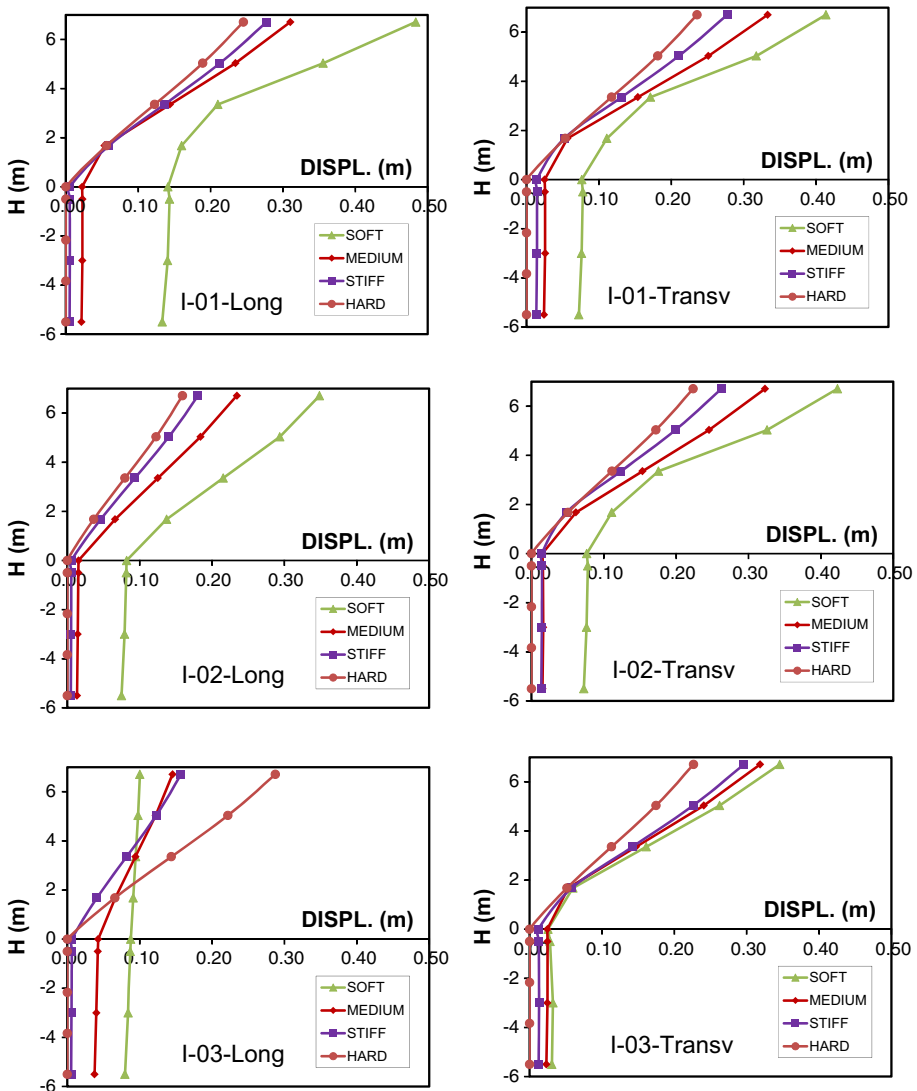
Fig. 15 Maximum column displacements (longitudinal and transversal directions)

Figure 15 shows the maximum column displacements in longitudinal and transversal directions for all the configurations and soil conditions. In particular, Fig. 15, I-03-Long plots the effect of non-linear isolators. In the case of soft condition, the soil is so deformable that it does not oppose any reaction to the displacements induced by the earthquake. Thanks to presence of the isolators at the top of the columns, the column can translate longitudinally without bending. Therefore, the final behaviour consists of a rigid translation of the entire pile shaft-bridge column system.

Table 4 shows maximum longitudinal and vertical displacements for the 100 earthquakes in correspondence with the top of the column. The resulting values support the role
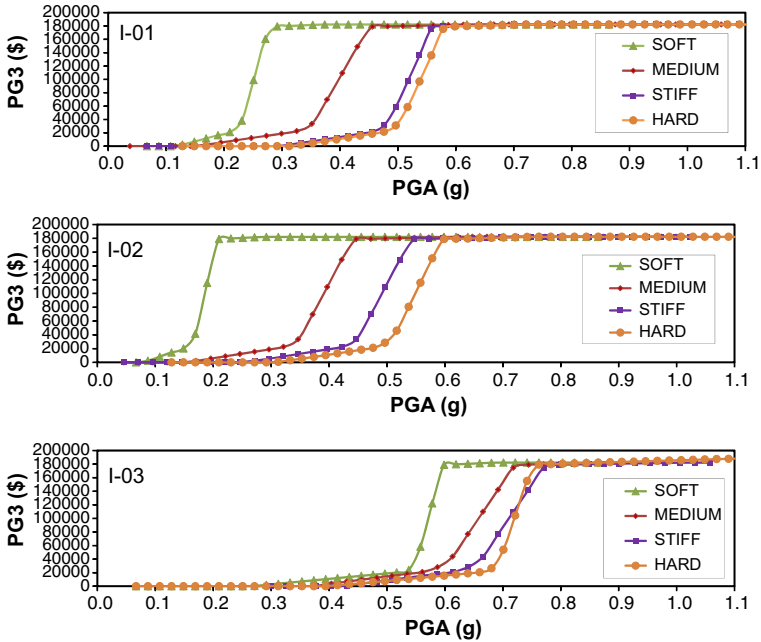
Fig. 16 Maximum longitudinal relative deck end–abutment displacement—PG3 Results

Table 4 Column maximum top displacements

	Hard			Stiff			Medium			Soft		
	Long (cm)	Tran (cm)	Vert (cm)	Long (cm)	Trans (cm)	Vert (cm)	Long (cm)	Tran (cm)	Vert (cm)	Long (cm)	Tran (cm)	Vert (cm)
I-01	24.53	23.56	1.36	27.74	27.72	1.52	31.02	33.32	1.85	48.36	41.38	4.58
I-02	15.92	22.34	1.26	18.06	26.26	1.45	23.44	32.28	1.76	34.86	42.29	5.19
I-03	17.54	22.67	1.29	11.76	29.63	1.66	9.58	29.39	1.96	6.11	35.92	3.01

of soil deformability on the three configurations. In particular, soft soil conditions are severe for I-01 model, were the performed displacement is 48.36 cm, considerably out of the limit state for isolator devices (design displacements: 37 cm, following ALGA specifications for HDS 650 × 337). Table 4 also shows isolation effect in reducing the longitudinal displacements, especially when non-linear devices are applied (I-03). The reduction is more effective in the longitudinal direction than in other directions.

Figure 16 shows that soil deformability is detrimental to all three configurations. Costs increase at lower values of PGA as soil deformability increases. This is due to the increase in abutment horizontal displacements and vertical settlements, as shown in Table 5. Comparing Tables 4 and 5, it is possible to assess that column isolation increases abutment deformations. In detail, the damage is transferred from the columns to the abutments. Therefore, I-02 model PG3 values are shown to be bigger that those relative to the I-01 model. In particular, the displacements obtained with soft soils are 83.45 and 97.97 cm for I-01 and I-02, respectively. These values have to be considered not acceptable within the

Table 5 Abutment maximum displacements

	Hard			Stiff			Medium			Soft		
	Long (cm)	Tran (cm)	Vert (cm)	Long (cm)	Trans (cm)	Vert (cm)	Long (cm)	Tran (cm)	Vert (cm)	Long (cm)	Tran (cm)	Vert (cm)
I-01	27.76	20.01	1.35	31.81	24.36	1.52	35.79	30.75	1.85	83.45	43.25	4.67
I-02	33.82	19.17	2.42	34.01	23.33	2.20	36.44	35.03	2.51	97.97	44.05	5.15
I-03	11.47	19.22	0.73	11.65	22.95	0.92	13.18	23.89	0.98	12.63	41.44	0.96

limit state for isolator devices (design displacements: 37 cm, following ALGA specifications for HDS 650 × 337). In these cases, the presence of deeper foundation or soil improvement can be a necessary countermeasure aimed at improving the whole bridge-ground system performance. On the other hand, when non-linear isolation is applied (I-03 model), there is a substantial reduction of deformations, especially in case of soft soil. In this case, displacement values can be considered acceptable because inside the limit state for isolator devices (design displacements: 40 cm, following ALGA specifications for APS 3000/800). Finally, soil deformability is more important for I-01 and I-02 than for I-03, where PG3 curves (and displacements) are closer to each other. This means that non-linear devices are able to decouple the abutments and the soil, performing their function.

Tables 4 and 5 show that, for I-01 model on hard soil, column and abutment displacements are similar. They increase when soil deformability increases and in correspondence with soft soil, abutment longitudinal displacements are bigger than those of the column. The effects of column isolation (model I-02) can be seen in a reduction of longitudinal displacements. On the contrary, abutment displacements are similar or even bigger than those performed in model I-01. In particular, for soft soil, column displacements are smaller while abutment longitudinal and vertical displacements increase, if compared with I-01 model. This is due to the fact that the settlements mainly affect the end of the deck while the column remains roughly vertical (due to its symmetric deformation). The I-03 model has small and similar column and abutment longitudinal displacements. Its effect consists of small longitudinal displacements for the deck and definitively that non-linear isolation improves system performance. Moreover, transversal displacements of the entire structure (column and abutments) increase with the soil deformability. In some cases, especially in correspondence with soft soil, transversal displacements become bigger than the longitudinal ones.

Figure 17 shows that, for I-03 on soft and medium soils, RCR increase starts at higher values if compared with I-01 and I-02 configurations. In particular, in case of soft soil, the values at which damage starts increasing are respectively 0.10 g for I-01 and I-02 models while 0.58 g for I-03 model. For stiff and hard soils, effects of non-linearity are particularly evident between 0.50 g and 0.70 g where RCR values are 25 % instead of 35 %. These results confirm the benefit of adopting sliding systems instead of traditional isolators. Figure 17 shows that soil affects the response in the range of PGA: 0.1–0.6 g for I-01 and I-02 and 0.3–0.8 g for I-03. In particular, soil deformability is detrimental to I-01 and I-02 models, since RCR increase is smoother for hard soil. For I-03 model, there is a level of PGA after which RCR reaches the same maximum value (RCR = 35 %). This level for soft and medium soils is around 0.60 g, while for stiff and hard ones, it is around 0.75 g. These values can be considered the points where soil deformability starts to become comparable with the shear strain imposed during seismic excitation and thus the influence of column damage starts to affect RCR (compare with Fig. 13). In this regard, the damage
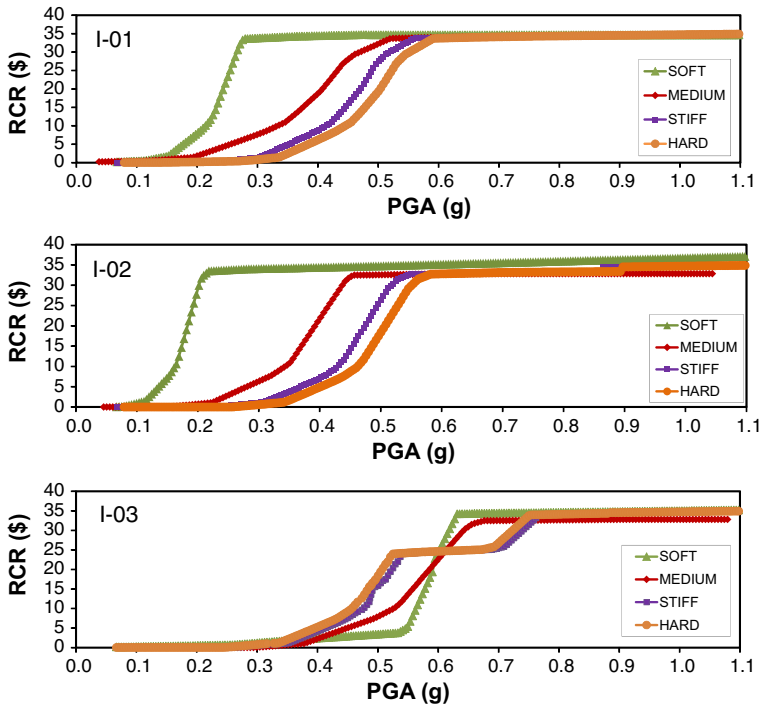
Fig. 17 Total repair costs (RCR)

can be reduced only increasing soil stiffness (for example with deep foundations or soil improvement). RCR equal to 35 % is reached for all the configurations, no manner which soil has been considered.

4 Conclusions

The study conducted in this paper may be viewed as an original contribution to seismic assessment of a benchmark bridge taking into consideration economic performance. In particular, isolation technique and SSI have been studied applying a PBEE approach.

The study aims at taking into account two sources of non-linearities. The first regards the soil. For this reason, several soils have been considered and the role of soil deformability has been assessed by considering the same bridge structure founded on different soils. On the other hand, isolator non-linearity has been considered as well. The mutual effect of soil and isolators non-linearities has been studied in order to assess the best isolated configuration able to fit the different non-linear conditions of the soil. In this regard, the study allows to understand that linear modelling of isolators and of the soil can result in incorrect evaluation of the problem.

Isolation technique is evaluated considering two isolation models representative of elastomeric bearings and frictional/sliding bearings. A parametric study on soil deformability has been performed in order to assess the circumstances under which SSI need to be considered. The selected soil profiles captured the effects of amplification and consequent

accumulation of ground deformation (laterally and vertically) thanks to OpenSees potentialities in soil modelling (in particular non-linearity and hysteretic damping). Results show that total costs are affected mainly by abutment damage and detrimental effects of soil deformability. The effects of different types of isolations have been evaluated. In this regard, the study assesses the benefit of non-linear isolators in protecting structural elements. Finally, this study can be considered one of the relatively few attempts to assess seismic behaviour of isolated bridge configurations considering economic performance. The outcomes of the present case study can contribute to SSI assessment for engineers and consultants.

Further analysis will aim to reproduce more sophisticated models for the isolators, taking into account their application in transversal direction that can significantly modify seismic responses.

References

Attewell P, Farmer IW (1973) Attenuation of ground vibrations from pile driving. Ground Eng 6(4):26–29

Bousshine L, Chaaba A, De Saxcé G (2001) Softening in stress–strain curve for Drucker–Prager nonassociated plasticity. Int J Plast 17(1):21–46

Caltrans (1994) The northridge earthquake. Post earthquake investigation report. Caltrans seismic design criteria version 1.3, California Department of Transportation, Sacramento, 2003

Chaudhary MTA, Abe M, Fujino Y (2001) Identification of soil-structure interaction effect in base-isolated bridges form earthquake records. Soil Dyn Earthq Eng 21:713–725

Dafalias YF (1986) Bounding surface plasticity I: mathematical formulation and hypoplasticity. J Eng Mech ASCE 112(9):966–987

Elgamal A, Yang Z, Parra E, Ragheb A (2003) Modeling of cyclic mobility in saturated cohesionless soils. Int J Plast 9(6):883–905

Elgamal A, Lu J, Forcellini D (2009) Mitigation of liquefaction-induced lateral deformation in sloping stratum: three-dimensional numerical simulation. J Geotech Geoenviron Eng 135(11):1672–1682

Elgamal A, Forcellini D, Lu J, Mackie KR, Tarantino AM (2012) A parametric study on several bridge-abutment configurations adopting a performance-based earthquake engineering methodology. In: II international conference on performance-based design in earthquake geotechnical engineering, Taormina, 28–30 May

Forcellini D (2014) Seismic assessment of soil structure interaction on several isolated bridge configurations adopting a PBEE methodology. In: Second European conference on earthquake engineering and seismology Istanbul, 25–29 Aug 2014

Forcellini D, Gobbi S (2015) Soil structure interaction assessment with advanced numerical simulations. In: Computational methods in structural dynamics and earthquake engineering (COMPDYN) conference, Crete Island, 25–27 May 2015

Forcellini D (2016) A direct-indirect cost decision making assessment methodology for seismic isolation on bridges. J Math Syst Sci 4(03–04):85–95. doi:10.17265/2328-224X/2015.0304.002

Forcellini D, Banfi M (2013) Case studies on several isolated bridge configurations adopting a performance based design approach. In: Proceedings of the 7th New York city bridge conference on durability of bridge structures, CRC Press, New York City. ISBN: 978-1-13-800112-1, pp 185–194

Forcellini D, Kelly JM (2014) The analysis of the large deformation stability of elastomeric bearings. J Eng Mech ASCE 04014036:1–10. doi:10.1061/EM.1943-7889.0000729

Forcellini D, Tarantino AM, Elgamal A, Lu J, Mackie K (2012) Seismic assessment of isolated bridge configurations on deformable soils adopting a PBEE methodology. In: Proceedings (N.260) of the 15th world conference on earthquake engineering, Lisbon, 24–28 Sept

Iwan WD (1967) On a class of models for the yielding behavior of continuous and composite systems. J Appl Mech ASME 34:612–617

Jesmani M, Fallahi AM, Kashani HF (2012) Effects of geometrical properties of rectangular trenches intended for passive isolation is sandy soils. Earth Sci Res 1(2):137–151

Kelly JM (1997) Earthquake-resistant design with rubber. Springer, Berlin

Kelly JM (2003) Tension buckling in multilayer elastomeric bearings. J Eng Mech ASCE 129(12):1363–1368

Ketchum M, Chang V, Shantz T (2004) Influence of design ground motion level on highway bridge costs. Report no. Lifelines 6D01, Pacific Earthquake Engineering Research Center, Berkeley, 2004

Kondner RL (1963) Hyperbolic stress-strain response: cohesive soils. J Soil Mech Found Div 89(SM1):115–143

Kramer SL (1996) Geotechnical earthquake engineering. Prentice Hall, Inc., Upper Saddle River, New Jersey, p 653

Kunde MC, Jangid RS (2003) Seismic behavior of isolated bridges: a state-of the art review. Electron J Struct Eng 3(2):140–170

Law HK, Lam IP (2001) Application of periodic boundary for large pile group. J Geotech Geoenviron Eng 127–10:889–892

Lee Z-K, Wu T-H, Loh C-H (2003) System identification on the seismic behavior of an isolated bridge. Earthq Eng Struct Dyn 32(14):1797–1812

Liao WI, Loh CH, Wan S (2000) Responses of isolated bridges subjected to near-fault ground motions recorded in Chi-Chi earthquake. In: Proceedings of international workshop on annual commemoration of Chi-Chi earthquake, vol II, pp 371–380

Lu J, Mackie KR, Elgamal A (2011) BridgePBEE: OpenSees 3D pushover and earthquake analysis of single-column 2-span bridges, User manual, beta 1.0. (http://peer.berkeley.edu/bridgepbee/)

Mackie KR, Stojadinovic B (2006) Fourway: a graphical tool for performance-based earthquake engineering. J Struct Eng 132(8):1274–1283

Mackie KR, Wong J, Stojadinovic B (2008) Integrated probabilistic performance-based evaluation of benchmark reinforced concrete bridges. Report No. 2007/09, University of California Berkeley, Pacific Earthquake Engineering Research Center, Berkeley

Mackie KR, Wong J-M, Stojadinovic B (2010a) Post-earthquake bridge repair cost and repair time estimation methodology. Earthq Eng Struct Dyn 39(3):281–301

Mackie KR, Lu J, Elgamal A (2010b) User interface for performance-based earthquake engineering: a single bent bridge pilot investigation. In: 9th US national and 10th Canadian conference on earthquake engineering: reaching beyond borders, Toronto, 25–29 July

Mackie K, Lu J, Elgamal A (2012) Performance-based earthquake performance-based earthquake assessment of bridge systems including ground-foundation interaction. Soil Dyn Earthq Eng 2(2012):184–196

Makris N, Zhang J (2004) Seismic response analysis of a highway overcrossing equipped with elastomeric bearings and fluid dampers. J Struct Eng 130(6):830–845

Mazzoni S, McKenna F, Scott MH, Fenves GL (2009) Open system for earthquake engineering simulation, user command-language manual. (http://opensees.berkeley.edu/OpenSees/manuals/usermanual). Pacific Earthquake Engineering Research Center, University of California, Berkeley, OpenSees version 2.0

Morgan TA, Mahin SA (2011) The use of base isolation systems to achieve complex seismic performance objectives. Report No. 2011/06, University of California Berkeley, Pacific Earthquake Engineering Research Center, Berkeley

Mroz Z (1967) On the description of anisotropic work hardening. J Mech Phys Solids 15:163–175

Nemat-Nasser S, Zhang J (2002) Constitutive relations for cohesionless frictional granular materials. Int J Plast 18(4):531–547

NGA database http://peer.berkeley.edu/nga/

Parra E (1996) Numerical modeling of liquefaction and lateral ground deformation including cyclic mobility and dilation response in soil systems. Ph.D. thesis, Rensselaer Polytechnic Institute, Troy

Prevost JH (1985) A simple plasticity theory or frictional cohesionless soils. Soil Dyn Earthq Eng 4(1):9–17

Radi E, Bigoni D, Loret B (2002) Steady crack growth in elastic-plastic fluid-saturated porous media. Int J Plast 18(3):345–358

Ryan KL, Kelly JM, Chopra AK (2005) Nonlinear model for lead-rubber bearings including axial-load effects. J Eng Mech 131(12):1270–1278. doi:10.1061/(ASCE)0733-9399(2005)

Thakkar SK, Maheshwari R (1995) Study of seismic base isolation of bridge considering soil structure interaction. In: Third international conference on recent advances in geotechnical earthquake engineering and soil dynamics, University of Missouri-Rolla, Rolla, vol 1, pp 397–400

Tongaonkar NP, Jangid RS (2003) Seismic response of isolated bridges with soil-structure interaction. Soil Dyn Earthq Eng 23(4):287–302

Ucak A, Tsopelas P (2008) Effect of soil-structure interaction on seismic isolated bridges. J Struct Eng 134(7):1154–1164

Vlassis AG, Spyrakos CC (2001) Seismically isolated bridge piers on shallow soil stratum with soil-structure interaction. Comput Struct 79(32):2847–2861

Yang Z, Elgamal A, Parra E (2003) A computational model for cyclic mobility and associated shear deformation. J Geotech Geoenviron Eng (ASCE) 129(12):1119–1127